



## Fault Detection and Diagnosis Based on Extensions of PCA

Y. Zhang<sup>\*</sup>, C. M. Bingham and M. Gallimore

*School of Engineering, University of Lincoln, Lincoln, U.K.*

The manuscript was received on 21 May 2013 and was accepted after revision for publication on 9 October 2013.

### Abstract:

*The paper presents two approaches for fault detection and discrimination based on principal component analysis (PCA). The first approach proposes the concept of  $y$ -indices through a transposed formulation of the data matrices utilized in traditional PCA. Residual errors (REs) and faulty sensor identification indices (FSIIs) are introduced in the second approach, where REs are generated from the residual subspace of PCA, and FSIIs are introduced to classify sensor- or component-faults. Through field data from gas turbines during commissioning, it is shown that in-operation sensor faults can be detected, and sensor- and component-faults can be discriminated through the proposed methods. The techniques are generic, and will find use in many military systems with complex, safety critical control and sensor arrangements.*

### Keywords:

*Fault detection, principal component analysis,  $y$ -index, residual error, faulty sensor identification index.*

### 1. Introduction

Fault Detection (FD) is an essential part in military control systems for operational reliability and safety. With regard to previously reported techniques for FD, principal component analysis (PCA) has been one of the most popular candidate solutions. An overview of traditional PCA is given below.

#### 1.1. Overview of Traditional PCA

PCA is extensively applied for data analysis purposes to reduce a large dataset whilst preserving 'sufficient' information contained in the original data [1]. Let  $\mathbf{X}$  be the original data matrix, with a mean 0.0 and a standard deviation 1.0.  $\mathbf{X} \subset \mathfrak{R}^{I \times J}$ , where  $I$

---

<sup>\*</sup> Corresponding author: Dr. Yu Zhang, School of Engineering, University of Lincoln, Lincoln, LN6 7TS, U.K. Tel: +44(0)1522 837938. E-mail: yzhang@lincoln.ac.uk

rows indicate the dimensions of data, i.e. the sensors, while  $J$  columns indicate the repetition of data from the experiment, i.e. the time steps. It can also be expressed as

$$\mathbf{X} = X_{ij}, \text{ where } i = 1, 2, \dots, I \text{ and } j = 1, 2, \dots, J. \quad (1)$$

The empirical covariance matrix,  $\mathbf{C} \subset \mathfrak{R}^{I \times I}$ , is derived using

$$\mathbf{C} = \frac{1}{J} \sum \mathbf{X}\mathbf{X}^T. \quad (2)$$

The eigenvectors and eigenvalues of the covariance matrix are found from

$$\mathbf{V}^{-1}\mathbf{C}\mathbf{V} = \mathbf{A}, \quad (3)$$

where  $\mathbf{V} \subset \mathfrak{R}^{I \times I}$ , with the  $I$  column vectors representing the  $I$  eigenvectors of  $\mathbf{C}$ , and  $\mathbf{A} \subset \mathfrak{R}^{I \times I}$  is the diagonal matrix of eigenvalues of  $\mathbf{C}$ , where  $A_{ij} = \lambda_k$  for  $i = j = k$  with  $\lambda_k$  as the  $k$ th eigenvalue of  $\mathbf{C}$ , and  $A_{ij} = 0$  for  $i \neq j$ . The eigenvectors and eigenvalues are rearranged in decreasing order. The cumulative sum of the variance for the  $i$ th eigenvalue is calculated from

$$s_i = \sum_{j=1}^i A_{jj} \text{ for } i = 1, 2, \dots, I. \quad (4)$$

Basis vectors are selected from a subset of the eigenvectors, while achieving a high value of  $s$  on a percentage basis, e.g.  $s_{\text{threshold}} = 95\%$ . When

$$\frac{s_{i=P}}{\sum_{j=1}^I A_{jj}} \geq s_{\text{threshold}}, \quad (5)$$

the first  $P$  columns of  $\mathbf{V}$  are used as the basis matrix  $\mathbf{V}_\alpha \subset \mathfrak{R}^{I \times P}$ , with  $V_{\alpha ij} = V_{ij}$  for  $i = 1, 2, \dots, I$  and  $j = 1, 2, \dots, P$ , where  $1 \leq P \leq I$ . To describe the original data in principal component space, the following relation is used:

$$\mathbf{Y} = \mathbf{V}_\alpha^T \mathbf{X}, \quad (6)$$

where  $\mathbf{X} \subset \mathfrak{R}^{I \times P}$  is the principal component matrix, which is a representation of  $\mathbf{X}$  after PCA, with the  $i$ th row representing the  $i$ th principal component. Since  $\mathbf{V}_\alpha$  is orthonormal, for any new input data sequence,  $\mathbf{x} \in \mathfrak{R}^{I \times 1}$ , an approximation of  $\mathbf{x}$  is:

$$\hat{\mathbf{x}} = \mathbf{V}_\alpha \mathbf{V}_\alpha^T \mathbf{x}. \quad (7)$$

Decomposing the data matrix into two parts, the principal component estimation part, and the residual part, gives

$$\mathbf{x} = \hat{\mathbf{x}} + \mathbf{e}, \quad (8)$$

where the residual can be expressed as

$$\mathbf{e} = (\mathbf{I} - \mathbf{V}_\alpha \mathbf{V}_\alpha^T) \mathbf{x}. \quad (9)$$

Principal components have been considered as the most important presentations in PCA, and have been used extensively for FD [2, 3].

### 1.2. Principal Components

Assume the original data matrix  $X$  is an  $I \times J$  matrix, the principal component matrix  $Y$  is an  $I \times J$  matrix, with the  $j$ th column an  $I \times 1$  interpretation of the original data for the  $j$ th sample. The first row of the principal component matrix is a  $1 \times J$  vector, which possesses the greatest variance in the original data. Therefore, the principal components, particularly the first, are often used for system monitoring and fault detection. For instance, [2] presented a framework based on PCA to detect real-time faults in an aluminium electrolysis process. When applying PCA, the principal component space defined by the first and third principal components is designated for FD. Abnormal events of the anode spikes are clustered in a distinct area, identified as the ‘problem area’, as shown in Fig. 1.

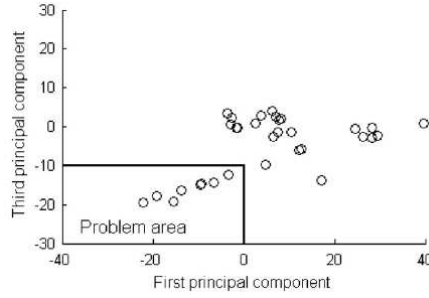


Fig. 1 First and third principal component plot for fault detection in aluminium electrolysis process [2]

In Fig. 1, the  $j$ th point represents the total behaviour of all variables (sensors) at the  $j$ th time step, through which it becomes useful for system monitoring. However, external algorithms are required in order to locate the ‘fault position’ (i.e. the faulted sensor).

### 1.3. Squared Prediction Error

Residuals generated by PCA are variances that are not captured in principal component space. When no faults are deemed to be present, they represent normal dynamics and noise present in the system, in the PCA residual sub-space. In the presence of a sensor fault, there is divergence of sensor correlations, and the residual vector deviates from the normal range. When a component fault occurs, excessive variance can be identified in the residual space, and the residual vector will also deviate out of the normal range.

According to (9), the squared prediction error (SPE) can be obtained from the predicted residual,  $e$ , as follows

$$SPE(x) = \|e\|^2 = x^T (\mathbf{I} - \mathbf{V}_\alpha \mathbf{V}_\alpha^T) x. \quad (10)$$

Here, the eigenvector matrix  $\mathbf{V}_\alpha$  is calculated from the previous data sets, i.e. the data history matrix, which is considered to be ‘normal’.

PCA based SPE, which is calculated in PCA residual sub-space, is well established and extensively applied for FD in process and power control [4-11]. Because SPE alone could not isolate the faulty sensor, additional algorithms are necessary for specific sensor fault identification (SFI). For instance, a sensor validity

index (SVI) was introduced for SFI in [4-8], and a SPE-contribution plot is presented as a supplement to SPE to diagnose sensor faults in [9, 10].

Paper [12] applied SPE for sensor fault detection (SFD) on a building energy management and control system subject to four fault cases, including (a) sensor bias, (b) drifting fault, (c) precision degradation and (d) complete failure, as shown in Fig. 2. For each time step, the value of SPE represented the variance in the residual sub-space after PCA for all the sensors. When SPE exceeded the threshold, it indicated abnormal behaviour data being read from the sensor.

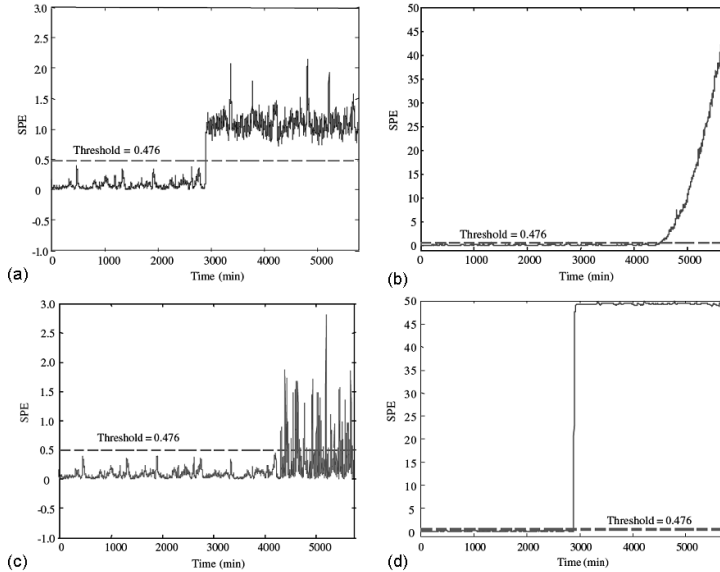


Fig. 2 Sensor fault detection by SPE [12]

However, such techniques require a 2-stage sequential procedure since SPE only provides results from an amalgamation of characteristics from the multiple sensors within the group. Moreover, SPE may not be directly suitable for systems where sensor data is subject to bias or drifting, for instance, which can be wrongly identified as representing a sensor or component fault.

#### 1.4. Concept of the Proposed Approaches

In the previous section, for both the principal component and SPE plots, each point in the plot represents the behaviour of all the sensors for one time step.

Here, a reformulation of principal component concept is proposed. Instead of looking for differences of a sensors' behaviour at different time steps, here, the focus is to investigate differences between sensors within a group. This can be achieved by performing PCA on the original data matrix  $X$  with a dimension of  $J \times I$ , where  $J$  is the number of samples, and  $I$  is the number of variables. The principal component matrix  $Y$  is a  $J \times I$  matrix, with the  $i$ th column a  $J \times 1$  interpretation of the original data for the  $i$ th sensor. The first principal component is the first row of the matrix, which is a  $1 \times I$  vector. In this way, for a designed time period, the differences between different sensors can be found from the first, or the first few  $1 \times I$  vectors, assuming it or they cover sufficient variances of the original data. A  $y$ -index is introduced that relates to

the first principal component, a  $1 \times I$  vector,  $y_1$ . A time-rolling window is used, as shown in Fig. 3. For each time step, a dataset for a total time  $t_b$  is studied by PCA, and  $I$  individually quantifiable numbers describe the differences between the  $I$  sensors in the sensor group. The resulting  $I$  representative characteristics are presented to the user on a rolling timeframe, showing changes in sensor behaviour that can be readily identified.

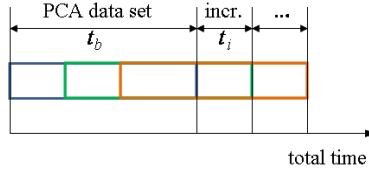


Fig. 3 The concept of PCA time rolling-in system

The second proposed approach is inspired by the traditional concept of PCA based SPE, and is developed in the residual sub-space in PCA. To employ traditional SPE methods, prior knowledge of the process is necessary, from which the SPE is then calculated for new data from eigenvectors obtained by PCA from the ‘normal’ operating data. To avoid this, here, the residual error (RE) is developed by calculating the residuals directly in real-time to monitor possible faults. As an alternative to the original SPE, therefore,  $\mathbf{R}$  is expressed as

$$\mathbf{R} = \mathbf{X}^T (\mathbf{I} - \mathbf{V}\mathbf{V}^T) \mathbf{X}, \quad (11)$$

where  $\mathbf{X}$  is the real-time data matrix after centring, with a dimension of  $I \times J$ . RE is calculated as the root-mean-square of the elements of  $\mathbf{R}$ , where the mean is obtained over  $J$  samples. RE brings benefits for system monitoring from direct data acquisition, where no prior knowledge is required.

In addition, where fault classification and identification is required, a faulted sensor identification index (FSII) is introduced, where the missing sensor method is used to calculate the difference between the principal component in the absence of the sensor, and with it included. FSII is used to check different sensors’ behaviour. If one FSII is significantly different from the others in the group, it is indicative of divergent behaviour. Combining REs and FSII thereby allows fault detection, classification and identification to be achieved.

The proposed ‘y-index’ method can be considered more robust than previously proposed techniques since:

- It can perform sensor fault detection and identification in one stage.
- Instead of investigating differences between a sensor’s behaviour implicitly as a function of time, the proposed method provides results relating to the differences of overall behaviour of a sensor with consideration of the behaviour of other sensors within the group.
- The proposed method is suitable for sensor fault detection in situations subject to bias and drifting during normal operation, where the results from traditional PCA methods can lead to excessive false alarms.

And the proposed ‘RE’ approach brings the following benefits:

- Unlike previous PCA based techniques, such as SPE method, which requires training datasets from historical process data to define the ‘normal’ behaviour, the proposed RE method is based on the residual space from real-time data.

- Whilst SPE is only suitable to detect faults for a process in steady state, RE is developed for fault detection in a quasi-steady process (processes without very dramatic transients).
- The moving window is designed to overcome the static analysis property of PCA and is applied to real-time (dynamic) data.

## 2. Methodology

### 2.1. Problem Statement

To provide an illustrative focus to the proposed methodology, a group of four vibration sensors sited on a twin shaft gas turbine is used (X and Y orientations on either end of a power turbine shaft), as shown in Fig. 4. Because of their relative positioning it has been observed that the data from these four sensors show qualitatively similar trends even when subject to situations involving unit components faults (as opposed to sensor faults). Practical examples of various conditions are shown in Fig. 5.

Three typical classes of sensor faults have been identified viz. those that exhibit transient ‘spikes’ in sensor readings (termed short faults); anomalous constant readings (termed constant faults); and long duration noisy readings (termed noise faults) [13], as shown, respectively, in Figs 5(b), (c), (d). These datasets are subsequently termed Test 1, Test 2 and Test 3, and are used to investigate the application of  $y$ -indices and RE techniques.

### 2.2. $Y$ -index

Assume the original data matrix  $X$  has a dimension of  $J \times I$ , where  $J$  is the number of samples and  $I$  is the number of sensors. The first principal component, a  $1 \times I$  vector,  $y_1$ , corresponds to the new axis with the greatest variances. The  $y$ -index is defined as the integer part of the square root of the distance between the absolute first principal component values, to describe the differences between the sensor reading data sets, and is expressed as:

$$d_y = \sqrt{|y_1| - \min(|y_1|)}, \quad (12)$$

where  $y_1$  is the first row vector of the principal component matrix, and  $|\bullet|$  refers to the absolute value. The greater the  $y$ -index, the more variance the particular sensor measurement contributes in the original data.

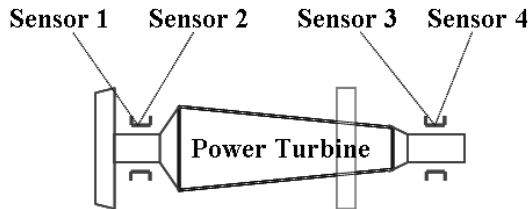


Fig. 4 The structure of four vibration sensors on power-turbine shaft

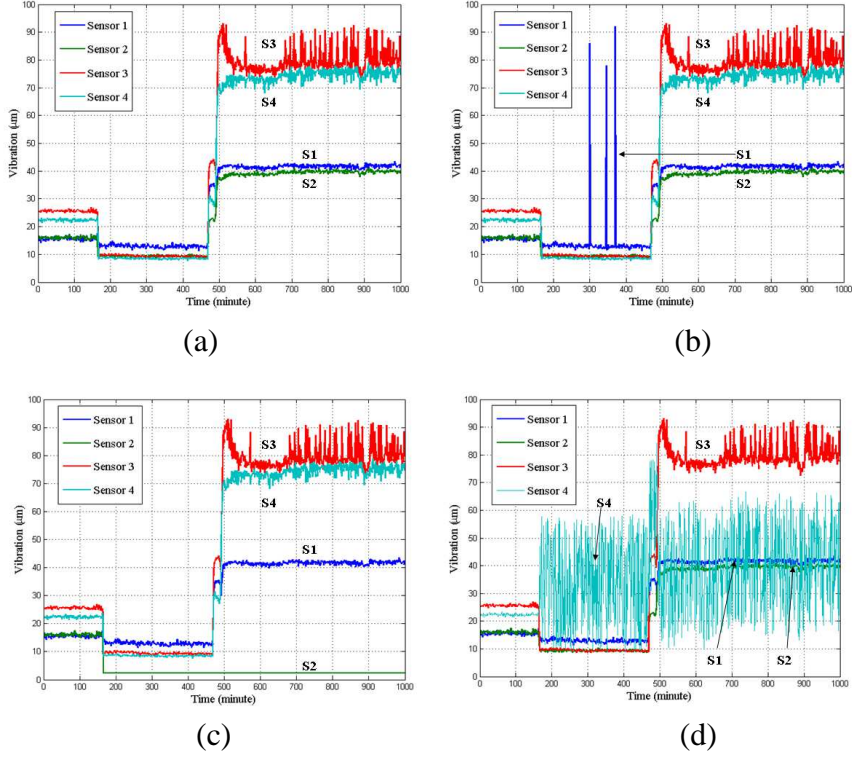


Fig. 5 Four sensor measurement characteristics during an emerging component failure: (a) original; (b) Test 1: Transient faults on Sensor 1; (c) Test 2: Constant reading fault on Sensor 2; (d) Test 3: Excessive noise fault on Sensor 4. ( $S$  = Sensor)

To check the efficacy of the  $y$ -index technique, Test 1 presents transient sensor faults on sensor 1, while data from the other three sensors are considered normal. Test 2 shows a constant-measurement fault on sensor 2, and Test 3 shows excessively noisy sensor data on sensor 4. Validation checks are carried out to calculate the errors  $e_1$  between  $y_1$  and  $y_c$ , and the errors  $e_2$  between  $d_y$  and  $d_{y_c}$ , in which  $y_c$  is the combined principal component vector that takes into consideration all the principal components in each row, and their variance contents, which contribute to the total variance of the original data. The combined principal component vector is then expressed as

$$y_c = \sqrt{(c_1 y_1)^2 + (c_2 y_2)^2 + (c_3 y_3)^2}, \quad (13)$$

where  $c_i$  is the variance content of the  $i$ th principal component and  $y_i$  is the  $i$ th row vector in the principal component matrix – see Tables 1, 2 and 3. Note: the term ‘PC’ refers to ‘principal component’,  $\lambda$  refers to the eigenvalue of the corresponding principal component, and  $s$  indicates the cumulative sum of the variances, from:

$$c_i = \frac{\lambda_i}{\sum \lambda_i} \quad \text{and} \quad s_i = \sum_{j=1}^i c_j \quad \text{where } i = 1, 2, 3. \quad (14)$$

Table 1 Validation check for Test 1

	$\lambda$	$c$ (%)	$s$ (%)
<b>PC1</b>	100.63	95.85	95.85
<b>PC2</b>	3.16	3.01	98.86
<b>PC3</b>	1.20	1.14	100.00

	$y_1$	$y_2$	$y_3$	$y_c$	$e_1$ (%)	$d_y$	$d_{yc}$	$e_2$
<b>Sensor 1</b>	14.93	0.33	0.02	14.31	4.15	3	3	0
<b>Sensor 2</b>	3.22	2.60	0.02	3.09	4.12	0	0	0
<b>Sensor 3</b>	5.76	1.17	1.34	5.52	4.15	2	2	0
<b>Sensor 4</b>	5.95	1.11	1.34	5.70	4.15	2	2	0

Table 2 Validation check for Test 2

	$\lambda$	$c$ (%)	$s$ (%)
<b>PC1</b>	521.78	98.32	98.32
<b>PC2</b>	7.74	1.46	99.78
<b>PC3</b>	1.16	0.22	100.00

	$y_1$	$y_2$	$y_3$	$y_c$	$e_1$ (%)	$d_y$	$d_{yc}$	$e_2$
<b>Sensor 1</b>	9.41	4.01	0.06	9.25	1.68	0	0	0
<b>Sensor 2</b>	34.20	0.26	0.01	33.63	1.68	5	5	0
<b>Sensor 3</b>	12.15	1.74	1.35	11.95	1.68	2	2	0
<b>Sensor 4</b>	12.63	2.01	1.28	12.42	1.68	2	2	0

Table 3 Validation check for Test 3

	$\lambda$	$c$ (%)	$s$ (%)
<b>PC1</b>	57.47	92.19	92.19
<b>PC2</b>	4.27	6.85	99.04
<b>PC3</b>	0.60	0.96	100.00

	$y_1$	$y_2$	$y_3$	$y_c$	$e_1$ (%)	$d_y$	$d_{yc}$	$e_2$
<b>Sensor 1</b>	1.47	0.53	0.36	1.36	7.78	0	0	0
<b>Sensor 2</b>	2.59	1.19	1.02	2.39	7.76	1	1	0
<b>Sensor 3</b>	5.38	2.41	0.26	4.96	7.76	2	2	0
<b>Sensor 4</b>	8.73	0.94	0.07	8.05	7.81	3	3	0

The errors are calculated using

$$e_1 = \frac{|y_1 - y_c|}{y_c} \times 100(\%). \quad (15)$$

$d_{y_c}$  is the  $y$ -index calculated from the combined principal component vector  $y_c$ , which is written as

$$d_{y_c} = \sqrt{|y_c| - \min(|y_c|)}. \quad (16)$$

Validation checks given in Tables 1-3 show that although there are errors (<10%) between the first row principal component vector and the combined principal component vector, for  $y$ -indices results, no difference exists between the two vectors. This shows a significant advantage for the efficiency of the  $y$ -index method. When the  $y$ -index is calculated, only the largest eigenvalue of the covariance matrix is considered to obtain the first row vector of the principal component matrix, and saves significant computational effort for the calculations of the remaining eigenvalues. Moreover, when plotted, the one-dimensional characteristic provides detection results graphically with respect to time.

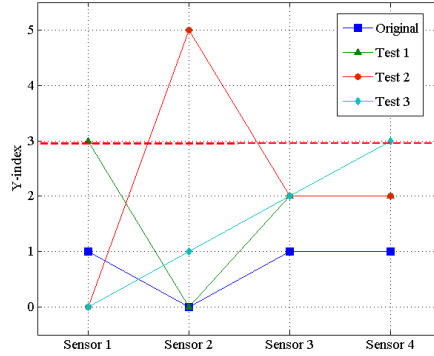


Fig. 6 The  $y$ -indices for the three test cases

For instance, the  $y$ -indices of the four sensors from the original data set, and three test cases, are presented in Fig. 6. The original data provides  $y$ -indices of four sensors to be 1, 0, 1, 1, which is considered as ‘normal’ sensor behaviour. From the results of using the other three test data sets, it can be seen that when the  $y$ -index is  $\geq 3$ , a sensor fault is considered to have occurred.

### 2.3. RE and FSII

An efficient adaption of the PCA-based algorithm is now used to detect and classify sensor- and component-faults. RE and FSII are both single quantifiable measures calculated from a PCA data set for each sensor. Thus, four representative characteristics can be presented using a ‘rolling window’ to identify qualitative changes in behaviour.

Assume  $X$  is the original data matrix with a dimension of  $I \times J$ , where  $I$  is the number of samples and  $J$  is the number of sensors. Recalling (11), the RE for the  $j$ th sensor is defined as:

$$RE_j = \sqrt{\frac{1}{I-1} \sum_{i=1}^I (X_{ij} - \hat{X}_{ij})^2}. \quad (17)$$

RE is used to detect abnormal conditions, i.e. unit component faults or sensor faults, during system operation. Abnormal behaviour is indicated when the RE migrates out of the normal range.

Since it is not possible for the sole use of the RE to distinguish between component- and sensor-faults, a further indicator, the FSII, is used. The proposed FSII is based on the traditional concept of the ‘missing sensor method’. Each row of principal components is calculated with- and without-the respective sensor, and the sum of squared differences is used for the FSII. Specifically, for the  $j$ th sensor:

$$FSII_j = \sqrt{\frac{1}{I-1} \sum_{i=1}^I (y_i - y_i^{(j)})^2}, \quad (18)$$

where  $y$  is the principal component vector computed in PCA.

*Tab. 4 REs for the three test cases*

	Original data	Test 1	Test 2	Test 3
Sensor 1	1.123	1.218	1.112	1.107
Sensor 2	1.147	1.158	1.496	1.129
Sensor 3	1.219	1.208	1.203	1.197
Sensor 4	1.226	1.216	1.211	1.214

*Tab. 5 FSIIs for the three test cases*

	Original data	Test 1	Test 2	Test 3
Sensor 1	0.073	0.805	0.001	0.001
Sensor 2	0.017	0.003	1.042	0.003
Sensor 3	0.041	0.007	0.001	0.048
Sensor 4	0.053	0.007	0.001	0.587

FSII is paired with the RE to classify component- and sensor-faults. When a sensor fault occurs, the FSII is also used to identify which sensor in the group is in error.

The REs and FSII of the four sensors from the original data set, and the three test cases, are listed in Tables 4 and 5. From the results, it can be seen that when the RE value is higher than  $\sim 1.2$ , both component faults (original data from sensors 3 and 4) and sensor faults (Test 1 from sensor 1, Test 2 from sensor 2, Test 3 from sensor 4) can be detected. According to the FSII table, it can be seen that, for a unit fault (original data), all the FSII approach a relatively low level, less than 0.1, and for sensor faults (Test 1-3), the FSII for the faulted sensor is much higher than those of the other sensors, where the FSII of the normally operating sensors’ approach zero.

### 3. Further Experimental Results

Using the rolling-window process depicted in Fig. 3, where the PCA data set  $t_b$  is taken as 1000 minutes, and the time increment  $t_i$  is set to be 30 minutes ( $t_b$  is pre-determined from the analysis of results from empirical trials, and  $t_i$  is designed according to a time delay that is considered acceptable for the application), the  $y$ -

index, RE and FSII, are applied to three field examples, covering both normal unit operation and operation when subject to known component and sensor faults.

### 3.1. Normal Operation

Example data sets from vibration sensors are shown in Fig. 7(a), taken from a randomly chosen field trial of normal unit operation, labelled as ‘Field Example 1’. It can be seen that the characteristics are not completely smooth and steady, but there are no sudden unexpected transients, or any apparent sensor measurement anomalies. The corresponding y-index is shown in Fig. 7(b), and the RE and FSII for this dataset are shown in Fig. 7(c).

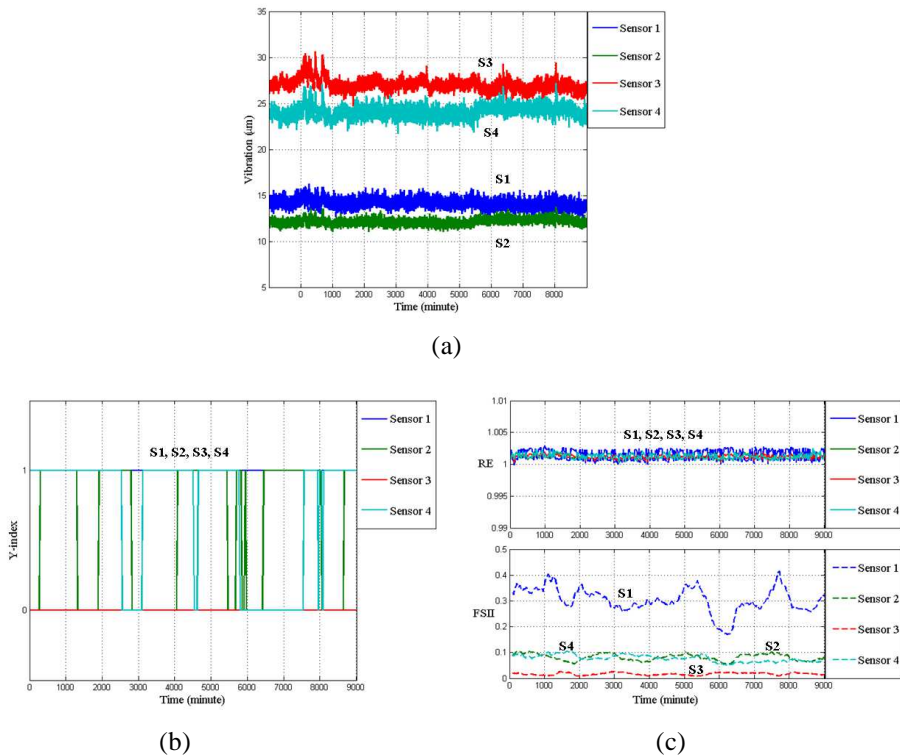


Fig. 7 Field Example 1: (a) Vibration measurements; (b) Y-index; (c) RE and FSII  
 ( $S = \text{Sensor}$ )

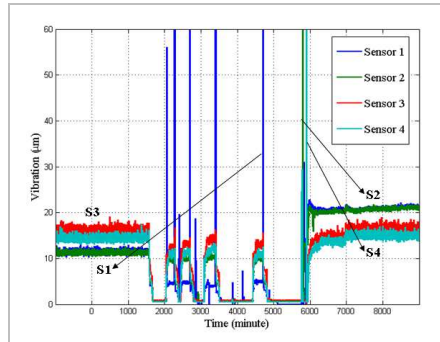
The y-indices continually show either 0 or 1, and no distinct increase of the RE is evident (the RE is much lower than 1.2). This would therefore be classified as ‘normal operation’ from the perspective of an operator (as expected). From site reports it is known that no sensor faults or unit component failures occurred during this period.

### 3.2. Sensor Fault Detection

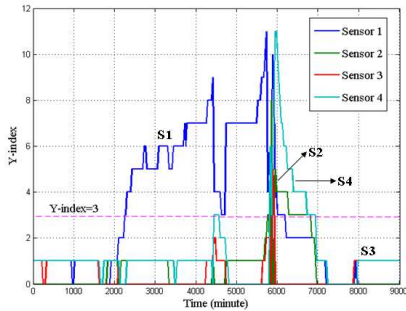
Fig. 8(a) shows real-time data with a sensor fault from the operational gas turbine, labelled as ‘Field Example 2’. Specific periods of interest are from 3000 to 6000 minutes, where a number of high-peak, ‘noisy’ readings from sensor 1 exist, and during the 6000 to 7000 minute period where a ‘high’ reading appears on sensor 2

measurements, and several high readings from sensor 4 exist (in practice a field engineer is performing sensor checks by swapping sensors during this time – in effect is creating anomalous conditions during unit operation).

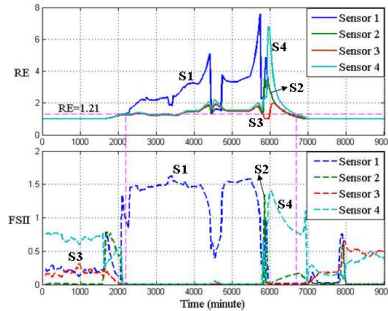
From Fig. 8(b), which shows the  $y$ -index plot for Field Example 3, it can be observed that, after collecting the data, the index line for sensor 1 rises to  $> 2$ . This is an indication of a potential sensor problem, and after further three time steps, the index exceeds the final warning value of 3, indicating that the operator should be alerted to check this particular sensor since it is showing anomalous characteristics compared to the rest. Notably, ‘the transient faults’ that occur on sensor 2 and sensor 4 in the time period of 5800 to 5900 minutes have also been correctly identified.



(a)



(b)



(c)

Fig. 8 Field Example 2: (a) Vibration information; (b)  $Y$ -index; (c) RE and FSII ( $S$  = Sensor)

Also, the sensor measurements ‘recover’ to normal behaviour i.e. within the range of values of 0 and 1, after 7000 minutes (which includes a delay of  $t_b$ , 1000 minutes), indicated by the indices becoming normal after the fault has been cleared.

From Fig. 8(c) it can be seen that the RE is out of range from 2100 to 6800 minutes. For this example, the RE shows a similar characteristic to the  $y$ -index output, with the fault being detected by both at around 2100-2200 minutes. From the FSII calculations, at 2200 minutes, the results for sensor 1 are much higher than those of the other sensors, with the FSII for the other sensors approaching zero. This identifies a sensor fault, and not a component fault, and classifies it as being on sensor 1. The

transient faults on sensor 2 and sensor 4 are also identified at ~5800 to 6000 minutes from the two peaks on the respective FSII plots at 5800 and 5900 minutes.

### 3.3. Component Fault Detection

High vibration and substantial mechanical transients can cause degradation of the turbine shaft bearings and potential damage to the unit. Fig. 9(a) shows an example of an emerging component fault, which occurs from around 4100 to 5100 minutes. After increasing transient amplitudes, high vibration readings occur on sensors 3 and 4. This example is termed ‘Field Example 3’. The corresponding y-index is plotted in Fig. 9(b), and the RE and FSII are plotted in Fig. 9(c). It can be seen that, for the short period during the emergence of the component fault, the y-indices increase to 2, but still does not exceed the limit of 3, which indicates that it is not a sensor fault. The corresponding RE plot shows data from sensors 3 and 4 remain beyond the limit during the emerging fault period and the FSII are all less than 0.1.

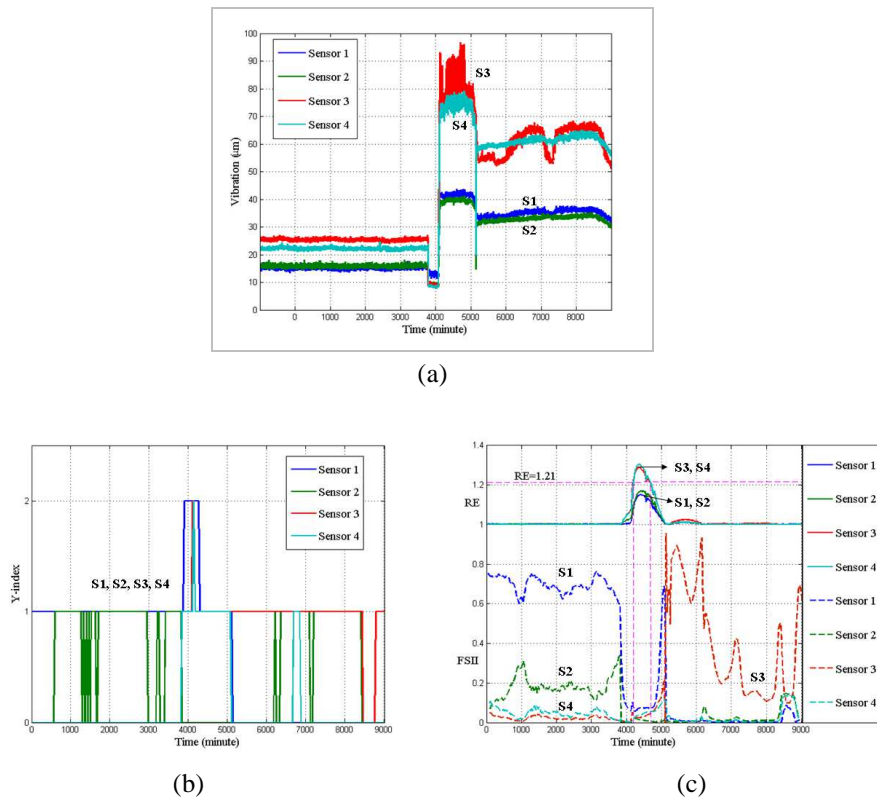


Fig. 9 Field Example 3: (a) Vibration information; (b) Y-index; (c) RE and FSII (S = Sensor)

RE’s ‘out of range’ is indicative of a fault emerging, and when the FSII all approach a common level, close to zero, it indicates that all the sensors are behaving consistently, evidencing a component fault as opposed to a sensor fault. It is also clear that the FSII have to be used in conjunction with the RE for fault detection, since the FSII are only indicative of how differently the sensors are behaving.

Overall, sensor- and machine-fault detection can be accomplished by noting:

- For normal operation,  $y$ -indices are showing 0s or 1s, and REs are much lower than the RE threshold;
- When sensor fault occurs,  $y$ -indices are higher than the threshold value 3, while REs are higher than the RE threshold value, and FSII of the faulted sensor are much higher than those of the normal sensors;
- When a highly-transient component fault occurs,  $y$ -indices remain lower than 3, but the REs are higher than RE threshold value, and FSII of all sensors approach zero.

#### 4. Conclusion

The paper has presented two readily implementable and computationally efficient approaches for FD using PCA based  $y$ -indices and REs. The  $y$ -indices are introduced by using transformed PCA input matrices, and are used to detect and identify sensor faults, while the REs and FSII are applied to detect and classify component- and sensor-faults. It has been demonstrated from various field data sets that a threshold for the  $y$ -index value of 3 is reasonable for encompassing the three categorized fault scenarios, and is investigated using experimental trials on gas turbine systems. The paired use of RE and FSII has been considered for component- and sensor-fault detection and discrimination. Initially, RE is used to detect abnormal operation conditions, which could be caused by either a transient change in measurement amplitudes or a sensor fault. Then, FSII is used to discriminate between component- and sensor-faults, and also to identify the faulted sensor (if one exists). The validity and efficacy of the proposed approaches have been demonstrated through the use of real-time operational data from gas turbine systems, and that in-operation sensor faults can be detected and identified by both proposed approaches. The techniques are generic, and could find use in many complex military systems with critical safety control requirements.

#### References

- [1] ABDI, H., WILLIAMS, LJ. Principal Component Analysis. *Wiley Interdisciplinary Reviews: Computational Statistics*, 2010, vol. 2, no. 4, p. 433-459.
- [2] MAJID, NAA., TAYLOR, MP., CHEN, JJJ., STAM, MA., MULDER, A. and YOUNG, BR. Aluminium process fault detection by Multiway Principal Component Analysis. *Control Engineering Practice*, 2011, vol. 19, no.4, p. 367-379.
- [3] COZZOLINO, D. and CURTIN, C. The Use of Attenuated Total Reflectance as Tool to Monitor the Time Course of Fermentation in Wild Ferments. *Food Control*, 2012, vol. 26, no. 2, p. 241-246.
- [4] DUNIA, R., QIN, SJ., EDGAR, TF. and McAVOY, TJ. Use of principal component analysis for sensor fault identification. *Computers & Chemistry Engineering*, 1996, vol. 20, suppl. 1, p. S713-S718.
- [5] YUE, HH. and QIN, SJ. Reconstruction-based fault identification using a combined index. *Industrial & Engineering Chemistry Research*, 2001, vol. 40, no. 20, p. 4403-4414.

- 
- [6] CHOI, SW., LEE, C., LEE, J-M., PARK, JH. and LEE, IB. Fault detection and identification of nonlinear processes based on kernel PCA. *Chemometrics and Intelligent Laboratory Systems*, 2005, vol. 75, no. 1, p. 55-67.
  - [7] XU, T. and WANG, Q. Application of MSPCA to sensor fault diagnosis. *Acta Automatica Sinica*, 2006, vol. 32, no. 3, p. 417-421.
  - [8] LEE, B. and WANG, X. Fault detection and reconstruction for micro-satellite power subsystem based on PCA. In *Proceedings of 3rd International Symposium on Systems and Control in Aeronautics and Astronautics 2010*, vol. 3, 2010. p. 1169-1173. ISSN 978-1-4244-6043-4.
  - [9] WANG, S. and XIAO, F. Detection and diagnosis of AHU sensor faults using principal component analysis method. *Energy Conversion and Management*, 2004, vol. 45, no. 17, p. 2667-2686.
  - [10] LIU, H., KIM, MJ., KANG, OY., KIM, JT. and YOO, CK. Sensor validation for monitoring indoor air quality in a subway station. In *Proceedings of 5th International Symposium on Sustainable Healthy Buildings 2011*, p. 477-489.
  - [11] NI, J., ZHANG, C. and YANG, SX. An adaptive approach based on KPCA and SVM for real-time fault diagnosis of HVCBs. *IEEE Transactions on Power Delivery*, 2011, vol. 26, no. 3, p. 1960-1971.
  - [12] WANG, S., CHEN, Y. Sensor Validation and Reconstruction for Building Central Chilling Systems Based on Principal Component Analysis. *Energy Conversion and Management*, 2004, vol. 45, no. 5, p. 673-695.
  - [13] SHARMA, AB., GOLUBCHIK, L. and GOVINDAN, R. Sensor Faults: Detection methods and prevalence in real-world datasets. *ACM Transactions on Sensor Networks*, 2010, vol. 6, no. 3, article no. 23.